Mine Water Environ (2015) 34:329–342
DOI 10.1007/s10230-015-0344-6

TECHNICAL ARTICLE

Metal Mobilization and Zinc-Rich Circumneutral Mine Drainage from the Abandoned Mining Area of Osor (Girona, NE Spain)

Andrés Navarro[1] · **Xavier Font**[2] · **Manuel Viladevall**[2]

Received: 13 January 2014 / Accepted: 5 May 2015 / Published online: 14 May 2015

Abstract Contaminated soil and mine wastes in Spain's abandoned Osor mining area contain Cd, Co, Pb, Zn, As, Ba, and Sb at levels that exceed Catalonia's regulatory limits for soils of industrial use. Mine water from the Coral adit, which is the main dewatering system in the Osor area, has circumneutral pH from carbonate and silicate dissolution, and high concentrations of Fe, Mn, Ni, Pb, and Zn. Geochemical modeling showed that smithsonite and hydrozincite were possible solid phases for Zn. The Coral adit is the main source of contaminants to Osor Creek, especially Zn and SO_4^{-2}.

Keywords Mine wastes · Leaching · Soils · Tailings · Geochemical modeling · Bioaccumulation

Introduction

Exploitation of F–Ba–Pb–Zn ores in the abandoned mining district of Osor (Girona, NE Spain) ceased in 1980 but has contaminated surface waters, groundwater, and soils in the vicinity of the main mine-waste impoundments. The main consequences of unremediated mine sites containing pyrite and pyrrhotite are the generation of acidic mine drainage waters and the possible mobilization of metals and metalloids (Lottermoser 2003; Plumlee et al. 1999). However, although less well documented, neutral mine drainage may also constitute a significant environmental problem due to the mobilization of metalloids such as As, Sb, Se, and metals such as Cd, Pb, and Zn (Heikkinen et al. 2009; Jang and Kwon 2011; Plante et al. 2011). The geochemistry of the mineral–water interaction depends on the ore and gangue minerals, local water chemistry, and geologic setting. Various types of mineral deposits tend to have distinct environmental signatures (Plumlee et al. 1999; Seal and Foley 2002; Seal and Hammarstrom 2003; Seal et al. 2008). Thus, the drainage water of polymetallic vein and related deposits that contain significant carbonate minerals in their gangue or wallrock alteration tend to have near-neutral pH, and elevated concentrations of Zn and Cu (Plumlee et al. 1999). Polymetallic replacement deposits hosted by carbonate sedimentary rocks tend to have mine water compositions with near-neutral pH and elevated concentrations of dissolved As, Fe, Sb, SO_4^{2-} and Zn (Al et al. 2000; Lee et al. 2005; Lindsay et al. 2009; Navarro et al. 2004; Navarro and Cardellach 2009; Plumlee et al. 1999). Also, elevated concentrations of Mn, Ni, and Fe in pore water from low sulfide tailings from Ni–Cu sulfide ores were documented by Heikkinen et al. (2009).

The neutral pH of the Osor mine water may be attributed to the dissolution of acid-consuming carbonate minerals associated with the carbonate gangue or host rocks. In some situations, precipitation of jarosite, gypsum, goethite, Fe oxy-hydroxides, siderite, and other secondary phases control Ca, Fe, Na, K, SO_4^{2-} and trace element concentrations (Blowes and Ptacek 1994; Blowes et al. 1998; Jurjovec et al. 2002; Navarro and Martínez 2010). Even when carbonate

Electronic supplementary material The online version of this article (doi:10.1007/s10230-015-0344-6) contains supplementary material, which is available to authorized users.

✉ Andrés Navarro
navarro@mf.upc.edu

[1] Department of Fluid Mechanics, School of Industrial and Aeronautical Engineering of Terrassa (ETSEIAT), Univ Politècnica de Catalunya, Colón 7–11, 08222 Terrassa, Spain

[2] Department of Geochemistry, Petrology and Geological Prospecting, Faculty of Geology, University of Barcelona, Zona Universitaria de Pedralbes, Barcelona, Spain

rocks host the affected aquifers, near-neutral groundwater may contain high dissolved concentrations of As, Fe, Ni, SO_4^{2-}, Zn, Cd, and Pb (Blowes et al. 1998; Ezekwe et al. 2013; Younger 2000). The main objectives of this study were to estimate metal mobilization and release of contaminants (especially Pb and Zn) from mine wastes based on laboratory and field tests. In addition, modeling was used to evaluate the chemical processes that may explain the geochemistry of the mine and surface water, and leachates.

Study Area

The abandoned Osor mining area (Fig. 1) lies some 35 km SE of Girona, in the La Selva basin and Montseny-Guilleries massif, which forms part of the Catalonian Coastal Range (CCR) in the NE section of the Iberian Peninsula. The main mineral deposits are in the Montseny-Guilleries massif and occur as stratabound and vein deposits associated with igneous and metasedimentary rocks of Paleozoic age (Fig. 1). These Paleozoic formations comprise the Lower Infra-Caradocian medium to high-grade metamorphic sequence, which can be divided into the high-grade Osor complex and the medium to low-grade Susqueda complex (Durán 1990; Reche and Martínez 2002), which are two pelitic series separated by orthogneiss.

Stratigraphically above lies the St. Martí Sacalm Caradocian volcano-sedimentary formation, the Silurian black slates, and the carbonatic Devonian St. Martí de Llémana formation. The Paleozoic shows a low and high-grade metamorphism (amphibolite facies) associated with the Variscan orogeny. The Paleozoic material was intruded by post-tectonic granitoids, mainly biotite granodiorites of calc-alkaline composition (Enrique 1990). Several mineralized veins that formed at low temperatures are found within the Paleozoic sequence (Canals and Cardellach 1997; Cardellach et al. 1990; Piqué et al. 2008). These include: Pb-rich veins of predominantly carbonate gangue (dolomite and ankerite) with significant vertical development that are enclosed exclusively within the Hercynian basement (south of the CCR); metal-poor and fluorite-rich veins that are also enclosed within the basement (Osor veins), and barite-rich veins that are associated with normal faults and minor amounts of sulfides (Bonmatí sector).

The main deposits exploited in this area were the stratabound polymetallic deposits of Pb–Fe–Ba in the Bonmatí sector (Fig. 1), associated with Susqueda Complex marbles and the F–Ba–Pb–Zn vein deposits of possible Jurassic age in the Osor area (Piqué et al. 2008). The Osor vein deposit is located 4 km SE of the town of Anglés, and includes several geologically similar and thick (1–4 m) fluorite-barite-sphalerite-galena veins, exploited to a depth of 300 m. Gangue minerals include quartz, barite, calcite, pyrite, and silicates (mainly muscovite, albite, and biotite). Exploitation of these veins concluded in 1980, after reaching annual productions of 20,000–30,000 t of fluorite,

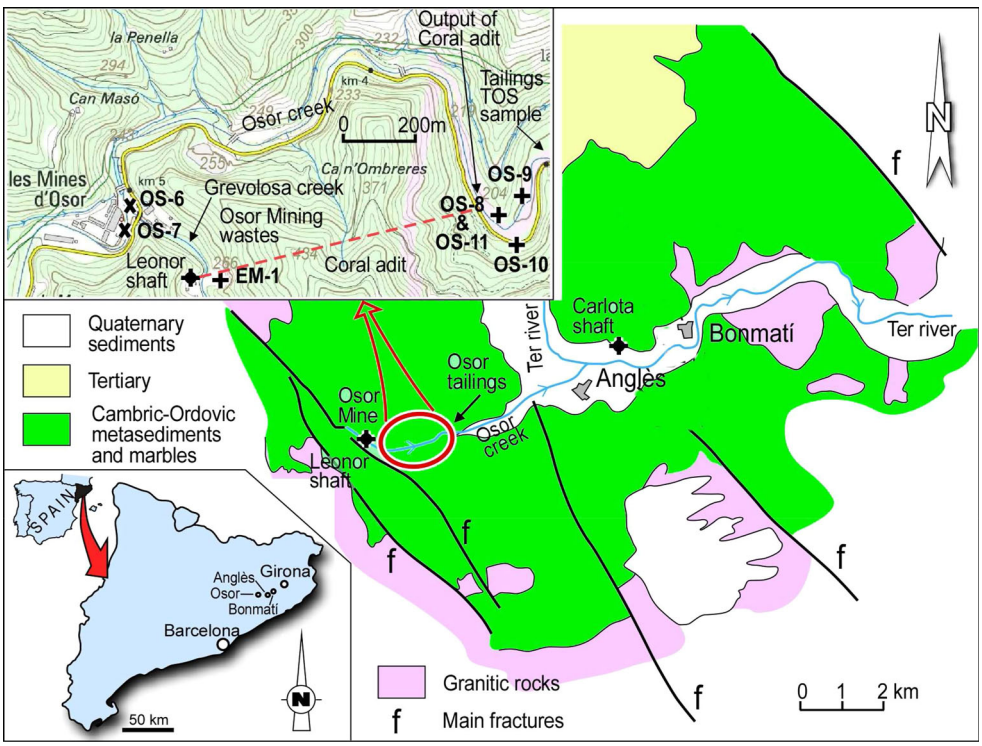

Fig. 1 Map of the study area showing a simplified geologic map and soil, mine wastes, and waters sampling points

2000 t of Pb concentrates, and 3000 t of Zn concentrates. The Osor flotation tailings were homogeneous in grain size and composition, occupying an area of 3150 m^2 with a mean thickness of 15 m and comprised a total affected volume of 60,000 m^3. Mine drainage was mainly through the Coral adit (Fig. 1), which drains the Osor vein system; it discharged an estimated 300 and 1100 m^3/day of near-neutral pH, contaminated mine water into Osor Creek. The mine water discharge was highest in the autumn and spring, and generally lowest in the late summer and early winter.

The studied area is characterized by a typically Mediterranean climate, with a mean annual rainfall of 736 mm and a mean annual temperature of 15 °C, with mean maximum and minimum temperatures of 21.1 and 9.5 °C, respectively. The only important water course in the area is the Ter River and its tributary, Osor Creek, which receives contaminated sediment and episodic draining waters from the Osor tailings area, and contaminated mine water from the Coral adit. Estimated mean discharge of the Ter River ranged from 3–15 m^3/s in the summer to 17–52 m^3/s in the wet period, mainly during early spring and fall.

Materials and Methods

Geochemistry and Mineralogy of Mineralization, Mine Wastes and Soil

The locations of the sampling sites are marked on Fig. 1. The Osor soils (OS-6, OS-7, OS-10, and OS-11) were sampled close (<3 m) to the water samples, including a sample of contaminated sediments of the Coral adit (OS-8) and stream sediments (OS-9). In the Osor mining area, flotation tailings (TOS sample) and mine waste dumps (sample EM-1) located close to the main extraction area (Leonor shaft) were sampled, together with ore samples from the outcropping vein system. Tree leaves from *Populus nigra* (black poplars) were also sampled from the bank of the Osor creek, at locations near the soil and water sampling points (O6 to O-10). *P. nigra* was used because of its efficiency in assimilating Co, Cr, Fe, Hg Sb, Cu, Ni, Pb, and Zn (Viladevall et al. 2007). Water, plant materials, soils, and wastes in the study area were characterized during four sampling campaigns conducted between 2009 and September 2010. Soil and mine wastes were collected with a plastic device and were stored and transported in hermetically sealed plastic bags.

Identification and analysis of the mineral phases in selected samples were performed in the University of Barcelona (UB) laboratories. We used X-ray diffraction (XRD) for selected samples. Once the materials had been dried and ground, the total concentrations of Au, Ag, As, Ba, Br, Ca, Co, Cr, Cs, Fe, Hf, Hg, Ir, Mo, Na, Ni, Rb, Sb, Sc, Se, Sn, Sr, Ta, Th, U, W, Zn, La, Ce, Nd, Sm, Eu, Tb, Yb, and Lu were determined using instrumental neutron activation analysis (INAA) in Actlabs (Ontario, Canada). In addition, the concentrations of the following elements were determined by acid digestion and subsequent analysis by inductively coupled plasma atomic emission spectrometry (ICP–AES): Ag, Cd, Cu, Mn, Mo, Ni, Pb, Zn, Al, Be, Bi, Ca, K, Mg, P, Sr, Ti, V, Y, and S. *P. nigra* samples were dried below 60 °C and macerated; then, a 15 g aliquot was compressed into a briquette and analyzed using INAA at Actlabs.

The grain size distribution of the mine wastes (sample EM-1) and tailings (sample TOS) was determined by sieving (RETSCH AS 200), the porosity by water displacement in a test tube, and field capacity by numerical methods.

Waters

Three surface water (OS-6, OS-7, OS-8), one spring (OS-10), and two mine water from the Coral adit (OS-8, OS-11) were collected between 2009 and 2010 (Fig. 1). Water sampling comprised four campaigns: winter 2009–2010 (OS-6 (W) to OS-10(W)), summer 2009 (OS-11(S)) and 2010 (OS-6(S) to OS-10(S)), and autumn 2010 (OS-6(A) to OS-10(A)).

The pH, redox potential (Eh), temperature, and electrical conductivity (EC) measurements were calibrated using standard solutions and measured in situ with portable devices (HACH model sensION TM378). The samples were filtered using a cellulose nitrate membrane with a pore size of 0.45 μm. The samples for cation analysis were later acidified to pH <2.0 by adding ultra-pure HNO_3. The samples were collected in 110 mL high-density polypropylene bottles, sealed with a double cap, and stored in a refrigerator until analysis. Metal concentrations were measured by inductively coupled plasma mass spectrometry (ICP-MS) at the ACTLABS laboratories. Concentrations of chloride, nitrate, and sulfate were analyzed on unfiltered samples, which were filtered with 0.45 μm filters in the laboratory by ion chromatography (IC). Water alkalinity was analyzed by titration with 0.01 HCl. Standard reference material NIST 1640 (ICPMS) was used to confirm accuracy. In order to preserve the carbonate equilibrium and CO_2 (g) levels in water samples, the samples were quickly closed and rapidly taken to the laboratory after sampling.

Flow-rate quantification of the Coral adit was performed during the water sampling using a broad-crested weir, which is a structure in an open channel that has a horizontal crest, above which the fluid pressure may be considered hydrostatic (Munson et al. 2009).

Column Leaching Experiments

Two column experiments were implemented to leach mining wastes and flotation tailings of the Osor sector (samples EM-1 and TOS, respectively). The column leaching method was a modified PrEN 14405 procedure, the standard European percolation test (SAIC 2003). We used a column that was: 750 mm long, 150 mm in diameter, and 5 mm thick. At the bottom of the column and attached to it was a plastic funnel that was 222 mm long with an internal diameter of 186 mm. Inside this was a fiberglass plate with holes in it, which acted as a support column. Methacrylate was coated onto a mesh that acted as a filter and retained the porous medium. Slightly mineralized water (SMW), similar to distilled water, was introduced into the column using a rain simulator connected to a metering pump. The experiments were carried out for 360 min with 6 leachates collected at the end of the column. The first leachates (TOS-1 and EM-1) was obtained after ≈60 min of pumping. In addition, in situ EC, Eh, and pH were measured.

To simulate the possible effects of rainfall on the ≈8.4 kg of tailings and ≈11.5 of mine wastes that packed the column, the system was designed so that the flow of water could be incrementally adjusted. A constant flow-rate of 1.31 L/h was used in the leaching experiments to simulate a typical precipitation event in this region. The filtration velocity obtained was 2.05×10^{-5} m/s and the pore velocity was 9.35×10^{-5} for the tailings and 6.64×10^{-5} for the mine waste. In addition, the pore volume in the column experiments was:

$$T_a = v \times t \times L^{-1} \quad (1)$$

where T_a is the number of pore volumes, v the pore velocity (m/s), t is the time of leaching (s), and L the column length (m). The final T_a was 5.46 pore volumes for the tailings and 4.62 for the mine wastes, indicating a time period that was considered representative.

Water samples were quickly sealed for anion analysis, and filtered, acidified, and sealed for metal analysis. Fluids were analyzed at Actlabs (Ontario, Canada) using IC to determine the dominant anions and using ICP-MS to analyze the following elements: Li, Na, Mg, Al, Si, K, Ca, Sc, Ti, V, Cr, Mn, Fe, Co, Ni, Cu, Zn, Ge, As, Se, Br, Rb, Sr, Y, Zr, Ag, Cd, Sn, Sb, Te, I, Cs, Ba, Hg, Pb, and REE. Results were compared to NIST reference sample 1640 to confirm accuracy.

Hydrogeochemical analyses of leachates were performed using the PHREEQC (Parkhurst and Appelo 1999) numerical code (version 3.0.6-7757) to evaluate the speciation of dissolved constituents and calculate the saturation state of the effluents. The MINTEQ thermodynamic database and the thermodynamic data of Preis and Gamsjäger (2001) were used for chemical equilibrium calculations.

Results and Discussion

Physical Parameters

The equivalent diameter of tailings and mine wastes were 1.5 and 6 mm, respectively. The bulk density and porosity of tailings were 1.29 g/cm^3 and 0.22, respectively, while the mine wastes had a bulk density of 2.1 g/cm^3 and a porosity of 0.31.

Mineralogy and Geochemistry of Ore, Mine Wastes and Tree Leaves

The mineralogical composition of the solid samples is given in Supplemental Table 1 (supplemental files accompany the on-line version of this paper, which can be downloaded for free by all journal subscribers and IMWA members). Quartz, fluorite, barite, calcite, galena, sphalerite, pyrite, albite, biotite, muscovite, and kaolinite were detected by XRD, binocular microscope, and visual inspection.

The mine waste sample from the Osor sector (EM-1) contained high amounts of Pb (>5000 mg kg^{-1}) due to the presence of argentiferous galena and high concentrations of Na, K, and Mg from silicates and possibly jarosite. The high Zn (11,300 mg kg^{-1}) and Cd (24.9 mg kg^{-1}) content could be associated with sphalerite, whereas the elevated Sb may be linked to galena or undetected sulfosalts. The Osor flotation tailings sample (TOS) contains high amounts of Al, Ba, and Sr due to concentration of gangue material in the flotation processes. Soil samples in the Osor area were comprised of alluvial soils (OS-6, OS-7, OS-10), stream sediment (OS-9) collected close to the water sampling locations (Fig. 1), and sediment deposited in the Coral adit (OS-8). Analysis of the sampled soils and sediments revealed As, Ba, Cd. Co, Sb, Pb, and Zn concentrations (Table 1) that exceed Catalonian soil intervention values.

Sample OS-8, associated with mine water in the Coral adit, contained higher amounts of As (121 mg kg^{-1}), Co (2540 mg kg^{-1}), Ni (506 mg kg^{-1}), Pb (3230 mg kg^{-1}), and Zn (71,000 mg kg^{-1}) than most other samples, and the highest amounts of Fe (7.75 %) and Mn (4.93 %). The amorphous character of this solid based on XRD suggests that it may be composed of Fe and Mn oxy-hydroxides that have sorbed high amounts of metals, and possibly hydrozincite ($Zn_5(OH)_6(CO_3)_2$) or an amorphous hydrated $ZnCO_3$ predecessor. Thus, the presence of As in the Coral

Table 1 Concentrations of metals and metalloids (in mg/kg, except for Al, Ca, and Fe, which are in %) in contaminated soils, ore samples, mine wastes, and vegetation

Element	D	UTM Coordinates	Al	Ag	As	Au	Ba	Bi	Ca	Cd	Co
DL	–		0.01	0.3	0.01	2	50	2	0.01	0.3	0.1
EM-1	0.3	466,412, 4,644,083	0.61	29.9	15.2	6	250	0.4	29.8	24.9	6
TOS	0.2	466,421, 4,644,434	4.46	0.6	12.5	<2	5110	0.3	7.33	7.6	14
Osor vein	sup	466,468, 4,644,095	0.24	66.2	164	32	2190	<2	21.4	68.5	15
soil OS-6	0.3	466,209, 4,644,283	6.48	3.5	5.7	<2	2200	<2	4.62	11.5	9
soil OS-7	0.3	466,182, 4,644,259	7.4	<0.3	3	<2	860	<2	0.61	<0.3	6
soil OS-8	0.3	467,203, 4,644,270	1.31	2.7	121	<2	<50	3	11.3	74.7	2540
soil OS-9	0.3	467,240, 4,644,241	7.01	<0.3	<0.5	<2	890	<2	0.66	<0.3	6
soil OS-10	0.3	467,215, 4,644,254	7.77	0.5	6.7	<2	900	<2	0.62	0.6	10
CAL*	–	–	–	–	30	–	1000	–	–	55	90
O-0	–	470,112, 4,645,612	ND	<0.3	0.6	5.7	50	ND	4.6	ND	3.4
O-6	–	466,203, 4,644,256	ND	<0.3	0.3	5.3	203	ND	4.7	ND	1.1
O-7	–	466,181, 4,644,221	ND	<0.3	0.4	17.6	173	ND	3.5	ND	1
O-8	–	467,147, 4,644,440	ND	<0.3	0.3	4.4	45	ND	3.8	ND	1
O-9	–	467,282, 4,644,225	ND	<0.3	0.4	5	195	ND	4.8	ND	1.5
O-10	–	467,318, 4,644,207	ND	<0.3	0.5	6.1	165	ND	4.1	ND	0.8

	Cr	Cu	Ni	Pb	Sb	Se	Sr	V	W	Zn	Hg	Mn	Mo	Fe
DL	0.3	1	1	1	0.005	0.1	1	2	0.05	1	0.05	1	0.05	0.01
EM-1	<2	11	3	>5000	56.5	<0.1	17	4	<1	11,300	3	89	<1	0.35
TOS	39	47	18	940	1	<0.1	105	45	<1	2370	<1	684	1	1.78
Osor vein	119	88	31	> 5000	208	<3	74	15	<1	34,000	5	109	1	0.96
OS-6	44	24	19	>5000	6.1	<3	109	48	<1	2730	<1	418	2	2.54
OS-7	14	9	6	22	0.2	<3	141	31	<1	79	<1	322	<1	2.11
OS-8	<2	18	506	3230	3.5	<3	103	13	15	71,000	<1	49,300	8	7.75
OS-9	22	9	8	55	0.5	<3	136	36	<1	114	<1	351	2	2.01
OS-10	45	19	23	50	0.4	<3	102	64	4	209	<1	519	<1	3.12
CAL*	1000	1000	1000	550	30	70	–	1000	–	1000	30	–	70	–
O-0	1.8	6	<1	1	0.06	0.4	110	ND	<0.05	53	<0.05	61	0.7	0.09
O-6	2.3	11	<1	15	0.11	<0.1	<10	ND	<0.05	974	0.35	81	0.56	0.02
O-7	1.5	5	<1	13	0.08	<0.1	120	ND	<0.05	589	0.22	144	<0.05	0.05
O-8	1.1	7	<1	4	0.06	<0.1	<10	ND	<0.05	982	<0.05	75	<0.05	0.01
O-9	0.0	9	<1	<1	0.06	<0.1	140	ND	<0.05	146	0.3	126	<0.05	0.03
O-10	1.1	6	<1	8	0.07	<0.1	<10	ND	<0.05	1220	0.29	31	0.32	0.01

D, depth of the samples; sup, superficial; CAL(*), the Catalonian soil intervention values (industrial use); EM-1, mining wastes; TOS, tailings; O-0 (control sample) to O-10: tree leaf of black poplar. ND, not determined; DL, detection limit

adit sediment may be associated with Fe oxy-hydroxides and the sorption of this metalloid by the amorphous oxy-hydroxides. In the alluvial soils from the Osor area, Ba, Pb, and Zn were only elevated in sample OS-6, which may have been collected above an old mine waste impoundment.

Tree leaf compositions reveal that all of the sampled plants have accumulated some metals (samples O-6 to O-10 in Table 1); the metal concentration in the samples collected from the Osor area exceed the concentrations detected in the reference sample (O-0) located in an uncontaminated area near the Ter river, close to the studied area. The recognition of accumulator plants was based on a comparison of the metal concentration in the plant to the metal concentration in the soil or the bioaccessible metal in the soil, using extraction techniques such as diethylene triamine pentaacetic acid (Lottermoser 2011). The samples analyzed indicated an accumulation of Au and Zn in the

leaves compared to the mean chemical composition of these metals in the Osor soils (Table 1). This comparison does not include the sediment of the Coral adit (sample OS-8) or the contaminated soil sample OS-6.

The mobility of Zn within plants varies depending on species, although Zn is likely to concentrate in mature leaves and in roots (13.9, 66.9 mg kg^{-1}, respectively) in plants cultivated close to mines (Kabata-Pendias and Mukherjee 2007). However, Zn concentrations in the tree leaves of black poplar in the studied area reach values of 146–1220 mg kg^{-1}, which is above the level that stops photosynthesis (178 mg kg^{-1}). Zn accumulation in these plants may be explained by the low content of several soil parameters in soils, such as phosphates, oxides, and organic matter that contribute to zinc retention in soils. The enrichment of Zn and Ni was similarly detected in several plants in the old Pb–Zn mining areas of the Aran Valley (Pyrenees, NE Spain) (Marques et al. 2003).

Water

Dissolved concentrations of major and minor components in the samples obtained during the summer and winter sampling campaigns were quite different (Tables 2, 3). The superficial waters were dominantly HCO_3–Ca, while the Coral adit water samples (OS-8, OS-11) had a HCO_3, SO_4-Ca composition (Fig. 2). The hydrogeochemical composition of the Coral adit (OS-8 and OS-11) and Coral spring (OS-10) samples (Tables 2, 3) suggests the weathering of similar materials. The mine water samples had higher metal levels and greater average alkalinity, from 40–45 to 290–377 mg/L (as HCO_3^-), indicative of sulphide oxidation and subsequent neutralization via carbonate dissolution.

Some samples exceeded the European Primary Drinking Water Regulations (EPDWR) for Mn, Fe, Ni, Pb, F, and SO_4 (Tables 2, 3). Fe and Mn clearly exceeded the EPDWR (50 and 200 μg/L, respectively), with the highest concentrations in the mine water samples (OS-8 and OS-11). Pb is possibly the contaminant of greatest environmental concern; three samples (OS-6 and OS-11) exceed the 10 μg/L EPDWR limit, even though Pb is relatively immobile in soils and groundwater because of its tendency to be adsorbed by Fe and Mn oxyhydroxides, and because of the low solubility of Pb sulphate and hydroxycarbonate. These Pb concentrations are similar to those detected in the old Pb mining district of La Carolina, Southern Spain,

Table 2 Metal and metalloid content (Na and Mg in mg/L; all else in μg/L) of water samples

Symbol	Na	Mg	Al	K	Ca	Mn	Fe	Co	Ni	Cu	Zn	As	Se	Cd	Ba	Pb
DL	0.005	0.001	2	0.03	0.7	0.1	10	0.005	0.3	0.2	0.5	0.03	0.2	0.01	0.1	0.01
OS-6 S	10.3	4.1	6	0.9	19.8	2.4	20	0.026	0.6	0.8	192	0.17	<0.2	0.57	32.4	13.6
OS-6 W	7.72	2.5	37	0.7	11.9	2.0	30	0.05	0.5	1.5	55.6	0.15	<0.2	0.14	20.2	3.63
OS-6 A	8.74	3.7	5	1	19.6	6	70	0.15	0.7	2.5	443	0.17	<0.2	1.19	36.8	36.7
OS-7 S	18.4	5.6	15	1.9	26.1	57.9	<10	0.05	0.7	2	34.4	0.58	<0.2	0.17	108	0.72
OS-7 W	17	3.9	23	1.3	19.5	14.9	50	0.05	1.1	2.1	23	0.31	<0.2	0.05	71.4	2.18
OS-7 A	19.1	4.5	5	2.1	33.4	10.4	80	0.05	0.8	2.8	152	0.4	<0.2	0.04	99.3	1.08
OS-8 S	34.9	19.8	4	5.1	134	879	<10	21.8	19.4	0.3	2800	0.6	0.3	2.47	39.9	2.61
OS-8 W	31.4	18	6	4.5	116	193	<10	3.66	15.1	0.6	>250	0.47	0.3	1.67	36.4	1.14
OS-8 A	28.7	16.4	3	4.3	135	749	240	20.1	17.9	2.8	2810	0.42	0.4	1.73	29.8	1.92
OS-11 S	42.5	28	49	6.2	189	1860	440	53.2	38.7	10.2	2800	2.2	<0.2	3.05	29.4	19.4
OS-9 S	19.6	7.6	11	2.3	42.2	141	20	2.33	3.6	2.3	1000	0.49	<0.2	0.39	90.8	1.69
OS-9 W	15.5	3.8	44	1.3	19.8	36.3	150	0.62	1.2	2.6	>250	0.32	<0.2	0.13	62	3.85
OS-9 A	21.8	8.9	5	2.7	74.2	226	90	5.61	5.9	2.5	1040	0.42	<0.2	0.54	69.4	1.39
OS-10 S	10	3.5	15	1.1	14	2.7	<10	0.034	0.4	1.2	25.3	0.14	<0.2	0.05	41.8	0.85
OS-10 W	9.74	3.6	16	1.3	14.2	10.6	70	0.28	0.7	1.7	>250	0.26	<0.2	0.06	42.5	2.46
OS-10 A	11.1	2.4	6	0.7	10	4.1	30	0.1	0.7	2.4	157	0.07	<0.2	0.04	33	0.74
EPDWR	200	–	200	–	–	50	200	–	20	2000	5000*	10	10	5	–	10

Sampling locations are provided in Table 2. ND, not determined; DL, detection limit; OS-6 (S,W,A), Grevolosa Creek (summer/winter/autumn); OS-7 (S,W,A), Osor Creek (summer/winter/autumn); OS-8 (S,W,A), Coral adit mine drainage (summer/winter/autumn); OS-9 (S,W,A), Osor Creek, downstream mine drainage (summer/winter/autumn); OS-10 (S,W,A), Coral spring (summer/winter/autumn); OS-11, Coral mine drainage (summer 2009); EPDWR, European primary drinking water regulations (maximum contaminant level)

* USA national secondary drinking water regulations

Table 3 Main anion contents of water samples; concentrations in mg/L; Eh in mV; EC in µS/cm; OS-6(S,W,A): Grevolosa Creek (summer/winter/autumn), OS-7 (S,W,A): Osor Creek (summer/winter/autumn), OS-8 (S,W,A): Coral adit drainage (summer/winter/autumn), OS-9 (S,W,A): Osor Creek, downstream mine drainage (summer/winter/autumn), OS-10 (S,W,A): Coral spring (summer/winter)/autumn, OS-11: Coral adit drainage (summer 2009)

Symbol	pH	Eh	EC	F	Cl	NO_3 (as N)	PO_4 (as P)	SO_4	HCO_3(−)	An. error (%)
Unit	–	mV	µS/cm	mg/L	mg/L	mg/L	mg/L	mg/L	mg/L	–
DL	–	–	–	0.01	0.03	0.01	0.02	0.03	1	–
OS-6 S	7.2	200	145	0.2	10	0.1	<0.02	8.8	72	3.3
OS-6 W	7.4	103	78.7	0.1	6.1	0.45	<0.02	8.7	45	1.3
OS-6 A	7.75	103	104	0.37	8.2	0.05	<0.02	8.3	96	1.2
OS-7 S	7.58	204	204	0.2	17	1.15	0.12	13	96	1.0
OS-7 W	8.21	60	141	0.1	18	1.57	0.09	11	60	4.9
OS-7 A	7.77	60	169	0.34	30.3	1.69	0.24	13.8	112	3.4
OS-8 S	7.68	197	950	1.9	28	<0.03	<0.06	180	324	1.7
OS-8 W	7.38	−2	860	2.1	26	<0.02	<0.04	156	290	6.0
OS-8 A	7.35	−2	563	2.31	26.9	<0.03	<0.06	171	293	0.49
OS-11 S	7.08	21	1180	2.1	29	<0.03	<0.06	288	377	5.3
OS-9 S	7.58	195	372	0.5	17	1.33	0.16	38	116	4.7
OS-9 W	7.3	60	159	0.2	16	1.37	0.06	13	61	7.9
OS-9 A	7.75	60	332	1.15	27.8	0.51	<0.04	71.7	186	3.1
OS-10 S	7.72	185	123	0.2	8.2	0.17	<0.02	18	40	1.9
OS-10 W	8.03	61	104	0.2	7.2	0.3	<0.02	18	45	0.7
OS-10 A	7.8	61	60.6	0.3	8.0	0.14	<0.02	18.7	41	4.0
EPDWR	–	–	2500	1.5	250	50	–	250	–	–

EPDWR, European primary drinking water regulations (maximum contaminant level); DL, detection limit; An. error, analytical error in %

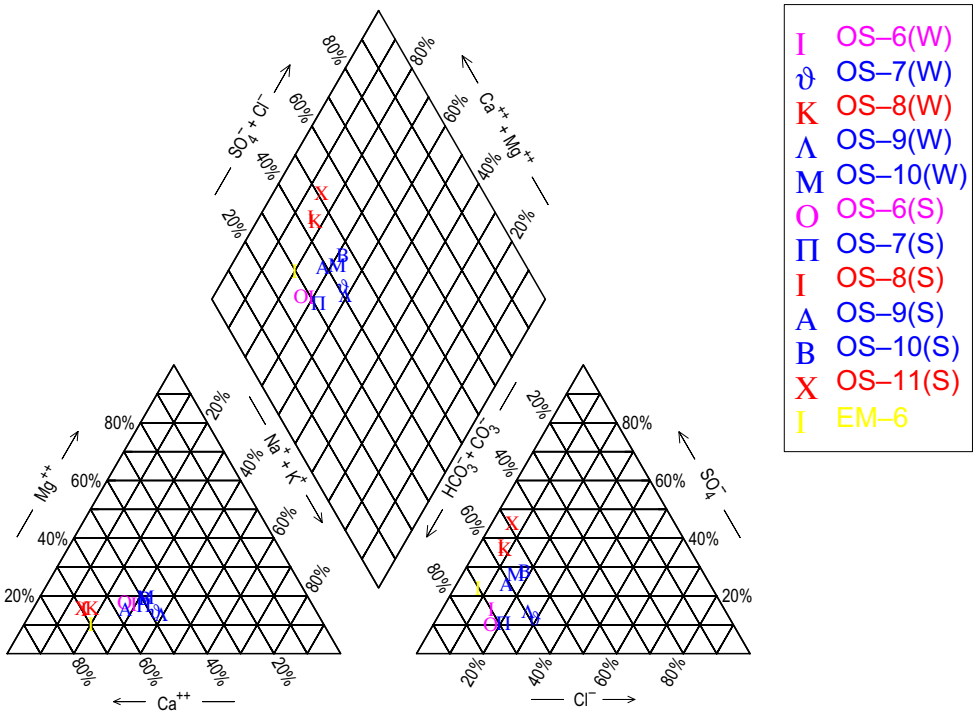

Fig. 2 Piper diagram of selected samples (superficial water, mine water, and leachate EM-6)

where mine water had a neutral pH and Pb concentrations between 0.6 and 850 μg/L (Hidalgo et al. 2010). The mobility of Pb in other abandoned mining areas, where waters had a circumneutral pH, was associated with the stability of $PbCO_3^0$ species at these pH conditions (Cidu et al. 2009). Also, concentrations of F (1.9 and 2.31 mg/L) in most of the impacted waters exceeded the EPDWR limit of 1.5 mg/L.

The mine water showed a direct relationship between high Zn and Cd content (Table 2). Zinc was generally the dominant base metal in the water samples, with concentrations up to 2.8 mg/L in the mine water, at a pH of 7.08–7.68. Metals such as Cd and Cu tended to increase with decreasing pH, although Cd still had significant concentrations at neutral pH, especially in the leachate samples. Ni showed a similar pattern, with higher concentrations at low pH and in the groundwater and leachate samples.

Oxyanion-forming elements such as As showed significant concentrations at neutral-alkaline pH conditions; lower concentrations were associated with lower pH (groundwater) samples and some samples with an elevated pH (superficial water samples). The lower As concentrations are likely associated with adsorption onto Fe oxy-hydroxide (Navarro and Domènech 2010).

Mine water samples (OS-8 and OS-11) showed high concentrations of Ca (116–189 mg/L), HCO_3 (290–377 mg/L), SO_4 (156–288 mg/L), and an elevated pH (7.08–7.68), which may indicate calcite dissolution in the Coral adit. The elevated concentration of SO_4^{-2} is most likely due to sulphide oxidation, although gypsum dissolution cannot be ruled out despite its absence in XRD analysis. Also, the elevated concentrations of Mn (0.19–1.8 mg/L) and Zn (up to 2.8 mg/L) suggest the dissolution of sphalerite and Mn oxides.

Moreover, the mine water had elevated concentrations of some cations, such as Na (31.4–42.5 mg/L), Mg (18.0–28.0 mg/L), and K (4.5–6.2 mg/L), above their concentrations in surface water and springs (Table 3), indicating that the weathering of some detected silicates (albite and muscovite) may have contributed to the high pH. Progress of the feldspar alteration reactions changes the activities of the dissolved solutes: Ca^{2+}, Na^+, K^+, H^+, $SiO_{2(aq)}$; thus, the albite and other aluminosilicates detected will not be stable in these waters and must dissolve (Appelo and Postma 1996):

$$2\ NaAlSi_3O_8 + 2H^+ + 9\ H_2 \rightarrow 2\ Na^+ + Al_2Si_2O_5(OH)_4 + 4H_4SiO_4 \quad (2)$$

$$NaAlSi_3O_8 + H^+ + H_2O \rightarrow Na^+ + Al(OH)_3 + 3H_4SiO_4 \quad (3)$$

Moreover, gibbsite [$Al(OH)_3$] is a weathering product of silicates, and dissolved Al may be associated with gibbsite dissolution. These neutralization processes and the relatively low quantity of pyrite may explain the elevated pH, and the mobility of metals such as Zn and Fe, resulting in low Fe concentrations in the mine water (OS-8 and OS-11, Table 2). Precipitation of Fe oxy-hydroxides was also observed at the Coral portal.

Leaching Experiments

Damköhler numbers were calculated in order to evaluate the factors that control mass-transfer in the column experiments and the proximity to equilibrium conditions. Damköhler numbers express the rate of reaction relative to advection or fluid flow rate; values over 10 indicate near-equilibrium conditions (Wehrer and Totsche 2003, 2005, 2008). The Damköhler number is expressed by:

$$D_a = x_{column} \times X_S^{-1} \quad (4)$$

where x_{column} is the length characteristic of fluid domain (column length filled with porous material) and X_S is the distance traveled after 63.2 % of the equilibrium is achieved (Grathwohl 2014). X_S may be evaluated from:

$$X_S = v \times \varepsilon / \left\{ \left(S_h \times D_{aq} / d_e^2 \right) \times (1 - \varepsilon) \times 6 \right\} \quad (5)$$

where v is the pore velocity, ε is the porosity, S_h is the Sherwood number, D_{aq} is the diffusion coefficient, d_e is the equivalent diameter of porous media, and the constant 6 is associated with spherical grains. Using Sherwood numbers between 7 and 10, the Damköhler number of the column experiments reaches values above 10, indicating a situation close to equilibrium conditions. In addition, the equilibrium time in the column experiments was evaluated from:

$$T_{eq} = \{ (x_{column}/v) \times R \times [1 - (X_S/x_{column})] \} \quad (6)$$

where T_{eq} is the equilibrium time and R is the retardation factor. For a retardation factor of 2, we find a T_{eq} of 131.5 min for tailings and 151.1 for mine wastes, indicating that equilibrium would be reached during the leaching tests.The continuous decrease of concentrations during steady state flow indicates that metal concentrations in the leachate (Figs. 3, 4) are controlled by availability rather than the solubility of pure mineral phases (Wehrer and Totsche 2008). Leachates from the Osor mine wastes (Table 4) showed pH values between 6.66 and 7.50 and EC values between 260 and 470 μS/cm. The most elevated EC values were associated with the Osor tailings leachates (TOS-1 and TOS-2). Zn was the metal that leached the best, with concentrations of 0.5–2.3 and 4.5–42.0 mg/L from the tailings and mining wastes, respectively (Table 4), which correlates with Zn being highest in the field.

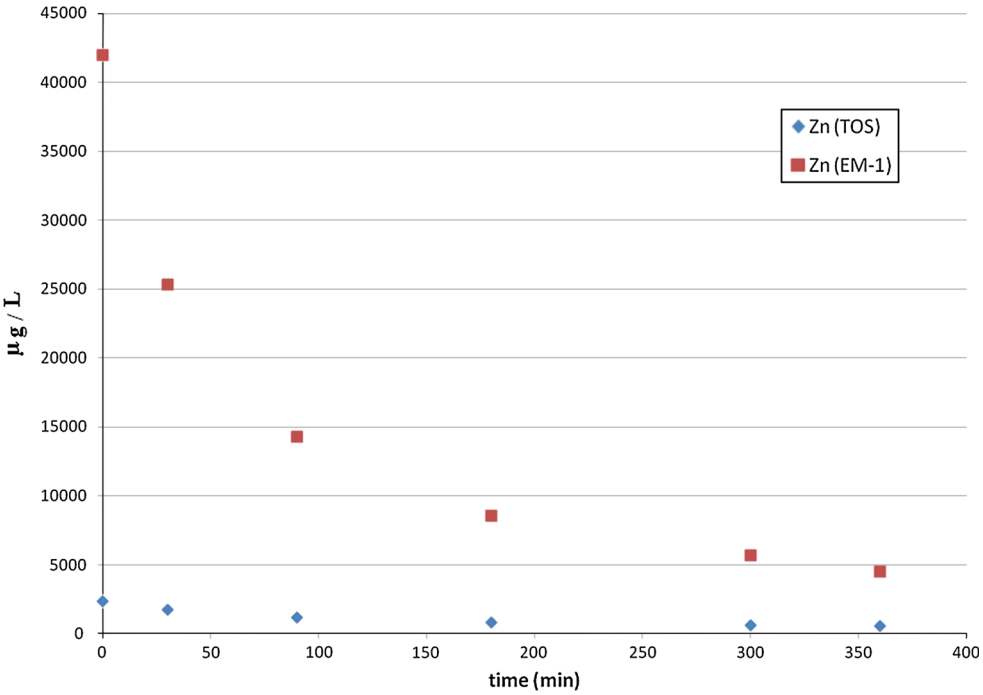

Fig. 3 Evolution of Zn with time for leaching experiments

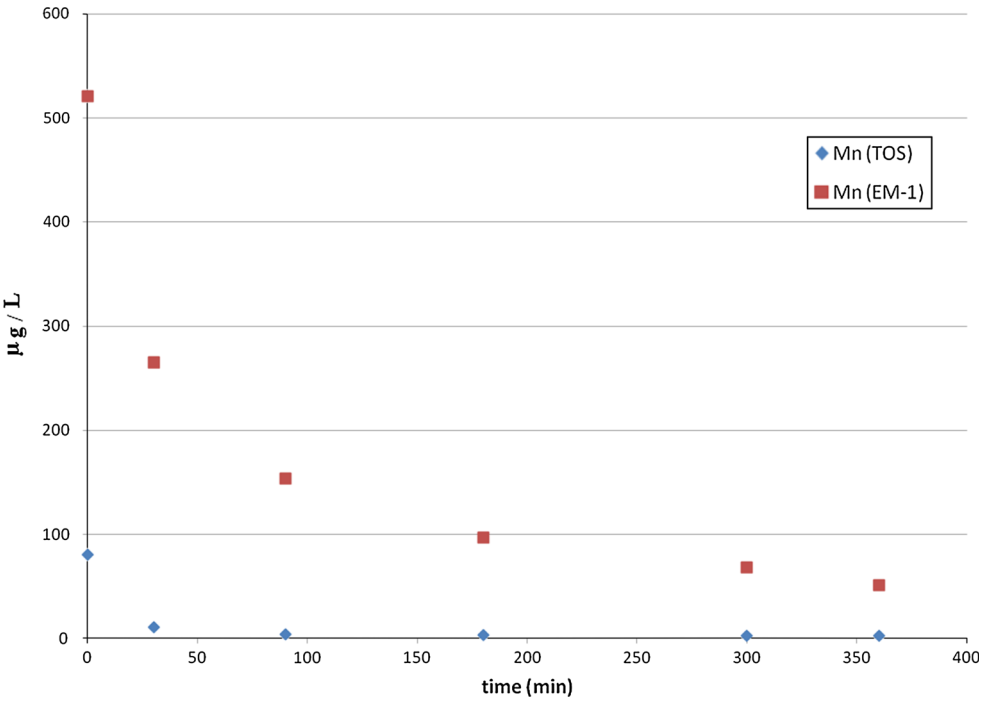

Fig. 4 Evolution of Mn with time for leaching experiments

Geochemical Modeling

Aqueous Speciation and Saturation State

PHREEQC was used on summer-water samples because they were, generally, the most mineralized fluids. It showed that the most abundant Fe species are Fe^{2+} and $FeSO_4$. The aqueous speciation of Pb was dominated by $PbCO_3^0$ with other species (Pb^{2+}, $PbHCO_3^+$, $PbOH^+$) lower by one or two orders of magnitude, similar to other Pb-contaminated areas (Navarro and Martínez 2010). The aqueous speciation of Zn showed that Zn^{2+} is the most abundant species. The remaining species ($ZnSO_4$, $ZnCO_3$, $Zn(CO_3)_2^{2-}$) are generally lower by one or two orders of magnitude.

The calculated saturation indices (SI) (Table 5) showed that most waters were saturated with respect to ferrihydrite and goethite, with the exception of the EM-1 leachate. Mine water sample (OS-11) and Grevolosa Creek (OS-6) were near equilibrium. On the other hand, waters and leachates were undersaturated with regards to Fe sulfate minerals and gypsum, with the exception of OS-11 (Coral adit drainage) which was close to equilibrium with jarosite, and the TOS-1 leachate (leachate from Osor tailings), which was oversaturated with regards to jarosite, jarosite-Na, and close to equilibrium with gypsum.

As for Pb and Zn minerals, all the water samples and leachates were undersaturated with anglesite, cerussite, and smithsonite. Only leachates EM-1 and TOS-1 (Table 5) showed SI values near equilibrium with respect to cerussite, which suggests possible control of dissolved Pb by $PbCO_3$. In addition, the mine drainage (OS-8 and OS-11) and EM-1 leachates were close to equilibrium with respect to smithsonite, which may indicate control of dissolved Zn by this mineral phase. However, another possible solid phase sink for Zn may be hydrozincite ($Zn_5(OH)_6(CO_3)_2$) which could precipitate via an amorphous hydrated $ZnCO_3$ predecessor (Younger 2000). Mine water samples from the Coral adit were saturated with respect to hydrozincite and near equilibrium (OS-11) with respect to $ZnCO_3{\cdot}H_2O$, although no crystalline Zn minerals were found in the Coral adit sediment.

Table 4 Main anion content (in mg/L) of leachate; time measured in minutes

	Time	F	Cl	NO_2 (as N)	Br	NO_3 (as N)	PO_4 (as P)	SO_4	HCO_3(−)
Detection limit	–	0.01	0.03	0.01	0.03	0.01	0.02	0.03	1
TOS-1	0	2.3	36.4	0.33	<0.6	34.3	<0.4	1790	72
TOS-6	360	3.86	6.57	<0.02	<0.06	0.4	<0.04	143	99
EM-1	0	3.72	40.7	<0.03	<0.09	1.48	<0.06	306	45
EM-6	360	3.27	7	<0.01	<0.03	0.43	<0.02	27	99
SMW	–	1.0	6.85	<0.01	<0.03	0.66	<0.02	10.9	99
MCL*	–	40	8500	–	–	–	–	7000	–

SMW, low mineralized water used in the leaching tests; MCL(*), maximum contaminated level of leachates (percolation test) of solid wastes, in order to deposit in landfills (inert solid wastes)

Table 5 Calculated saturation index for water samples and leachates

Mineral phase	OS-(S)	OS-7(S)	OS-8(S)*	OS-9(S)	OS-10(S)	OS-11(S)*	EM-1	TOS-1
Iron oxyhydroxides								
$Fe(OH)_3$	0.30	1.00	1.05	1.18	1.10	0.76	−2.08	1.97
Goethite	4.44	5.13	5.18	5.32	5.23	4.90	2.08	6.13
Sulphate minerals								
Jarosite	−4.72	−3.2	−0.79	−1.7	−3.18	0.34	−6.45	3.97
Jarosite-Na	−7.15	−5.68	−3.62	−4.24	−5.70	−2.28	−9.17	0.58
Gypsum	−2.72	−2.47	−0.92	−1.86	−2.54	−0.65	−1.00	0.24
Lead minerals								
Anglesite	−5.52	−6.28	−5.32	−5.55	−5.80	−3.79	−1.43	−2.40
Cerrusite	−2.12	−2.52	−1.96	−2.15	−2.46	−1.12	−0.23	−0.44
Zinc minerals								
Smithsonite	−1.94	−2.31	−0.17	−0.81	−2.60	−0.54	−0.50	−0.81
$ZnCO_3{\cdot}H_2O$	−1.61	−1.97	0.17	−0.48	−2.26	−0.20	−0.17	−0.48
Hydrocincite	29.4	28.4	37.9	35.6	28.5	34.3	35.7	37.1
Carbonate and other minerals								
Calcite	−2.72	−0.52	0.65	−0.27	−1.00	0.22	−1.59	0.40
Dolomite	−1.12	−1.52	0.67	−1.08	−2.40	−0.18	−3.79	0.23
Siderite	−2.27	−2.29	−1.83	−1.88	−2.53	−0.52	−2.87	−0.54
Gibbsite	0.05	0.34	−0.28	0.21	0.29	0.82	−1.17	1.46
SiO_2 (amor.)	−1.19	−1.34	−1.28	−1.23	−1.23	−1.22	−1.4	−1.74
Kaolinite	4.16	4.45	3.31	4.4	4.55	5.63	1.3	5.85

Saturation indices calculated using PHREEQC and database MINTEQ. * Coral adit. EM-1, TOS-1: leachates

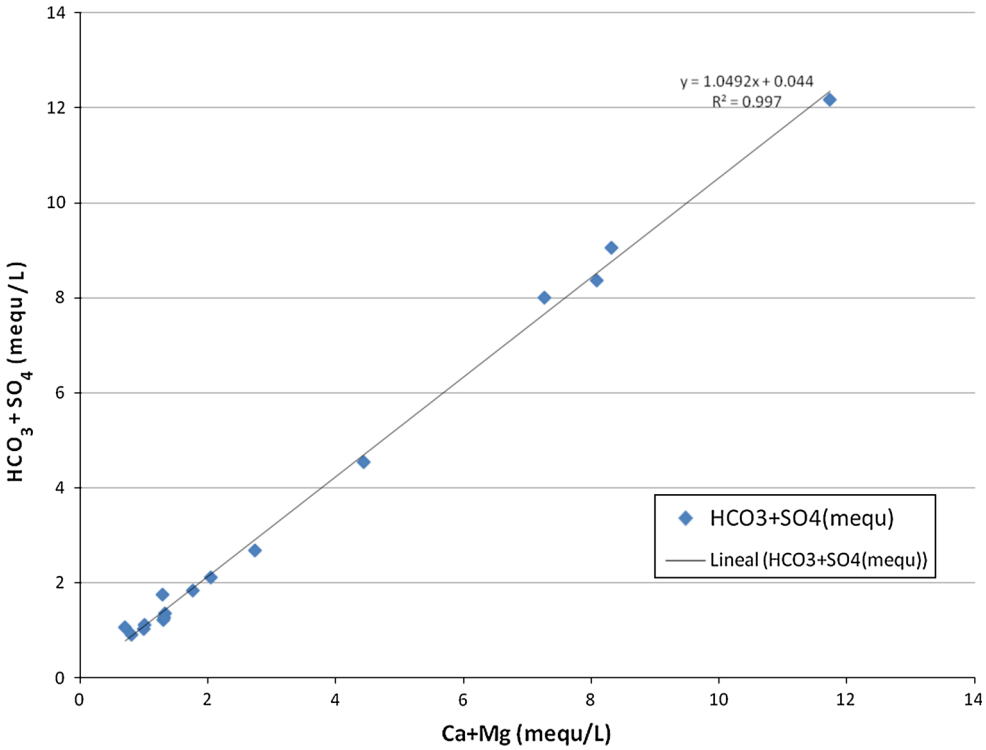

Fig. 5 (Ca + Mg) versus (HCO_3 + SO_4) scatter diagram of water samples

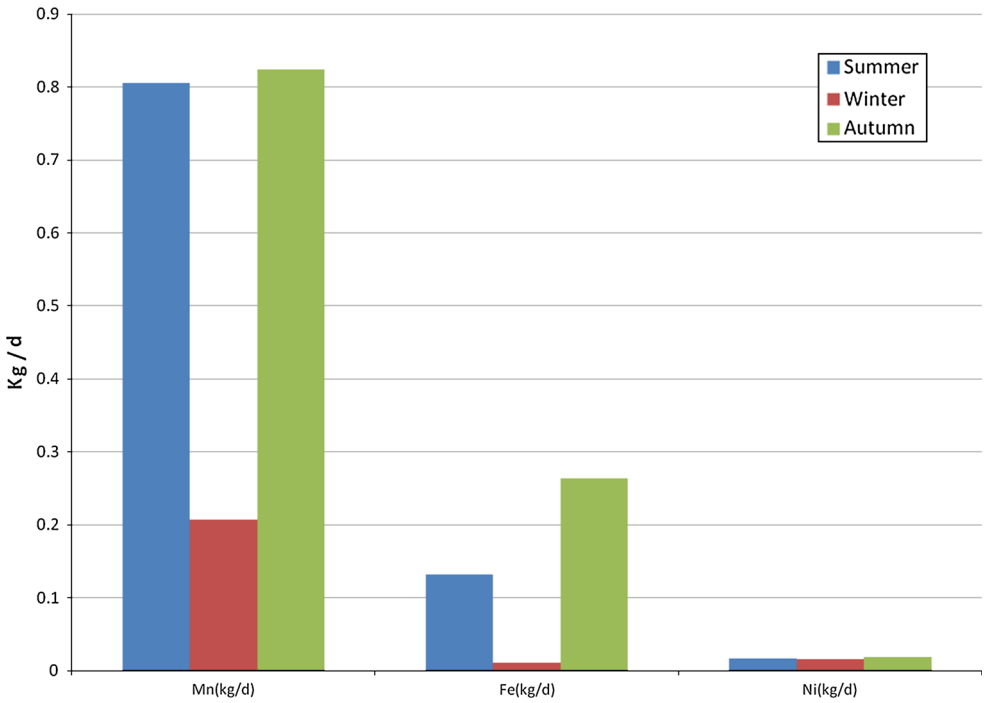

Fig. 6 Mn, Fe, and Ni mobilization from Coral adit to Osor Creek in summer, winter, and autumn

Furthermore, the carbonate minerals calcite, dolomite, and siderite were undersaturated in almost all of the samples, although near equilibrium in a leachate sample (TOS-1) and mine drainage waters (OS-8 and OS-11). Also, the SI of gibbsite, which was present in all of the samples with the exception of the leachates, was close to equilibrium, suggesting that this mineral phase controls the concentrations of dissolved Al. The (Ca + Mg) versus (HCO_3 + SO_4) scatter diagram follows the principle that ionic concentrations falling above the equiline may result from carbonate weathering, while those falling along the equiline are due to both carbonate and silicate weathering

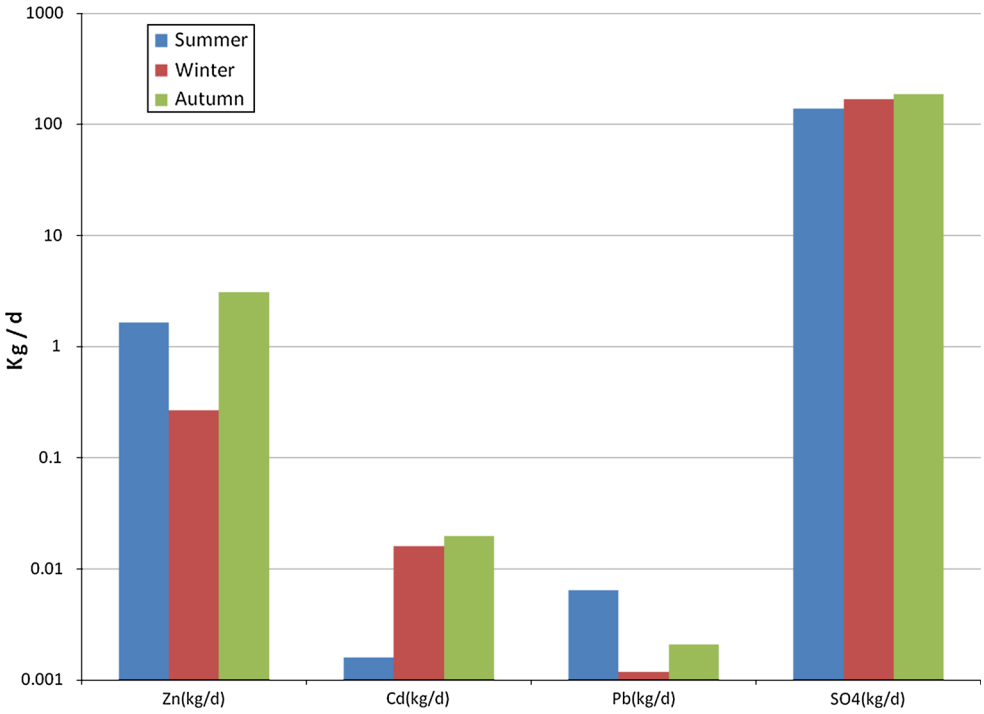

Fig. 7 Zn, Cd, Pb, and SO_4^{-2} mobilization from Coral adit to Osor Creek in summer, winter, and autumn

(Elango and Kannan 2007). Most of the Osor water samples lie along the equiline, which could indicate the weathering of carbonates and silicates (Fig. 5). The Eh–pH conditions of the leachates and water were consistent with these data, with the most stable species for Fe, Pb, and Zn being oxy-hydroxides of Fe, cerussite, and Zn^{2+}.

Evaluation of Metal Mobilization

Metal mobilization from the main potential source, the Coral adit, was evaluated from flow-rate measurements and contaminant concentrations in the adit water samples. The main contaminant flow from the Coral adit to the Osor Creek was evaluated using the mathematical expression of contaminant mass-flow:

$$M = \int C_0 V\ n\ dA \qquad (7)$$

where M: contaminant mass-flow (kg/day); C_0: mean contaminant concentration (kg/m^3); V: volume of mine water (m^3); n: elemental vector; dA: differential surface element (m^2), and; $\int V\ n\ dA$: adit flow-rate (m^3/day).

The mean concentrations of samples OS-8(S) and OS-11(S) were used to evaluate the seasonal contaminant mass-flow for summer production. The flow rate of the Coral adit was evaluated from discrete measurements, with a mean value of 837 m^3/day, equivalent to 305,700 m^3/year.

The mobilization of Mn, Fe, and Ni is shown in Fig. 6. Mn production reached values near 0.8 kg/day in summer and autumn, while low quantities of Fe and Ni were mobilized. Figure 7 illustrates that 1–3 kg/day of Zn was produced in summer and autumn. Mobilization of SO_4^{-2} was also very high, with a calculated production of 137–188 kg/day. However, Cd and Pb mobilization was low, although Pb production may reach 0.006 kg/day in summer.

Conclusions

Past mining in the Osor area has contaminated soil, sediment, groundwater, and surface water, despite the neutral character of the mine water. Mine wastes from the Osor sector contained high amounts of Pb (>5000 mg kg^{-1}), Zn (11,300 mg kg^{-1}), and Cd (24.9 mg kg^{-1}), which are possibly associated with sphalerite. The Osor tailings sample had high concentrations of Al, Ba, and Sr due to the gangue and soil composition. The concentrations of As, Ba, Cd. Co, Sb, Pb, and Zn in the sediment samples exceed the Catalonian soil intervention values.

Mine water samples had elevated concentrations of Ca (116–189 mg/L), HCO_3 (290–377 mg/L), and SO_4 (156–288 mg/L). The dissolved SO_4^{-2} is likely due to sulphide oxidation, although gypsum dissolution is thermodynamically possible; however, gypsum was not found in the ore and mine wastes samples. The mine water had an elevated pH (7.08-7.68), which may indicate calcite dissolution in the Coral adit. In addition, the elevated concentrations of Mn (0.19-1.8 mg/L) and Zn (>0.25–2.8 mg/L)

suggest the dissolution of sphalerite and Mn oxides. The mine water also had elevated concentrations of some cations, such as Na (31.4–42.5 mg/L), Mg (18.0–28.0 mg/L), and K (4.5–6.2 mg/L).

Column leaching experiments showed that the metal concentrations in the leachate are controlled by the availability rather than the solubility of mineral phases. The most released metal was Zn, which showed concentrations of 0.5–2.3 and 4.5–42.0 mg/L in tailings and mining wastes, respectively, which coincides with the most abundant metal in waters.

Geochemical modeling of mine waters and leachates indicated that some waters were close to equilibrium with respect to smithsonite, which may indicate control of dissolved Zn by this mineral phase. However, another possible solid phase sink for Zn could be hydrozincite.

The flow rate of the Coral adit was inversely related to EC and some dissolved cations (Na, Mg, K, Mn, Co, Cd, and Pb), which may just be due to dilution. The main environmental concern in this area is the mobilization of Zn and SO_4^{2-} by the Coral adit, estimated at 0.26–3.0 kg/day and 137.6–188.1 kg/day, respectively. This is a significant quantity of Zn and SO_4^{2-}, which flows into and contaminates Osor Creek.

Acknowledgments The research was supported by the Consolidated Research Group on Economic and Environmental Geology and Hydrology at the University of Barcelona (UB), with financial support (project SGR2005) from the Catalan Agency for the Administration of University and Research Grants (AGAUR). The authors also thank the anonymous reviewers.

References

Al TA, Martin CJ, Blowes DW (2000) Carbonate-mineral/water interactions in sulfide-rich mine tailings. Geochim Cosmochim Acta 64(23):3933–3948

Appelo CAJ, Postma D (1996) Geochemistry. Groundwater and Pollution, Balkema

Blowes DW, Ptacek CJ (1994) Acid-neutralization mechanisms in inactive mine tailings. In: Jambor JL, Blowes DW (eds) The environmental geochemistry of sulfide mine-wastes. Mineralogical Association of Canada Short Course Handbook, Canada

Blowes DW, Jambor JL, Hanton-Fong CJ (1998) Geochemical, mineralogical and microbiological characterization of a sulphide-bearing carbonate-rich gold-mine tailings impoundment, Jouetl, Québec. Appl Geochem 13:687–705

Canals A, Cardellach E (1997) Ore lead and sulphur isotope pattern from the low-temperature veins of the Catalonian Coastal Ranges (NE Spain). Miner Depos 32:243–249

Cardellach E, Canals A, Tritlla J (1990) Late and post-Hercynian low temperature veins in the Catalonian Coastal Ranges. Acta Geol Hisp 25:75–81

Cidu R, Bidau R, Fanfani L (2009) Impact of past mining activity on the quality of groundwater in SW Sardinia (Italy). J Geochem Explor 100:125–132

Durán H (1990) El Paleozoico de les Guilleries. Acta Geol Hisp 25(1–2):83–103

Elango L, Kannan R (2007) Rock-water interaction and its control on chemical composition of groundwater. In: Sarkar D, Datta R, Hannigan R (eds) Developments in environmental science. Elsevier, Amsterdam

Enrique P (1990) The Hercynian intrusive rocks of the Catalonian Coastal Ranges (NE Spain). Acta Geol Hisp 25:39–64

Ezekwe IC, Ezekwe AS, Chima GN (2013) Metal loadings and alkaline mine drainage from active and abandoned mines in the Ivo River basin area of southeastern Nigeria. Mine Water Environ 32:97–107

Grathwohl P (2014) On equilibration of pore water in column leaching tests. Waste Manag 34:908–918

Heikkinen PM, Räisänen ML, Johnson RH (2009) Geochemical characterization of seepage and drainage water quality from two sulphide mine tailings impoundments: acid mine drainage versus neutral mine drainage. Mine Water Environ 28:30–49

Hidalgo MC, Rey J, Benavente J (2010) Hydrogeochemistry of abandoned Pb sulphide mines: the mining district of La Carolina (southern Spain). Environ Earth Sci 61:37–46

Jang M, Kwon H (2011) Pilot-scale tests to optimize the treatment of net-alkaline mine drainage. Environ Geochem Health 33:91–101

Jurjovec J, Ptacek CJ, Blowes DW (2002) Acid neutralization mechanisms and metal release in mine tailings: a laboratory column experiment. Geochim Cosmochim Acta 66(9):1511–1523

Kabata-Pendias A, Mukherjee AB (2007) Trace elements from soil to human. Springer, Berlin

Lee JY, Choi JC, Lee KK (2005) Variations in heavy metal contamination of stream water and groundwater affected by an abandoned lead-zinc mine in Korea. Environ Geochem Health 27:237–257

Lindsay MBJ, Condon PD, Jambor JL, Lear KG, Blowes DW, Ptacek CJ (2009) Mineralogical, geochemical, and microbiological investigation of a sulfide-rich tailings deposit characterized by neutral drainage. Appl Geochem 24:2212–2221

Lottermoser B (2003) Mine wastes. Springer, Berlín

Lottermoser B (2011) Colonisation of the rehabilitated Mary Kathleen uranium mine site (Australia) by *Calotropis procera*: toxicity risk to grazing animals. J Geochem Explor 111:39–46

Marques AF, Queralt I, Carvalho ML, Bordalo M (2003) Total reflection X-ray fluorescence and energy-dispersive X-ray fluorescence analysis of runoff water and vegetation from abandoned mining of Pb-Zn ores. Spectrochim Acta B 58:2191–2198

Munson BR, Okishi TH, Huebsch WW (2009) Fundamentals of fluid mechanics, vol 6. Wiley, Hoboken

Navarro A, Cardellach E (2009) Mobilization of Ag, heavy metals and Eu from the waste deposit of Las Herrerías mine (Almería, SE Spain). Environ Geol 56(7):1389–1404

Navarro A, Domènech LM (2010) Arsenic and metal mobility from Au mine tailings in Rodalquilar (Almería, SE Spain). Environ Earth Sci 60:121–138

Navarro A, Martínez F (2010) Evaluation of metal attenuation from mine tailings in SE Spain (Sierra Almagrera): a soil-leaching column study. Mine Water Environ 29:53–67

Navarro A, Collado D, Carbonell M, Sánchez JA (2004) Impact of mining activities on soils in a semi-arid environment: Sierra Almagrera district, SE Spain. Environ Geochem Health 26:383–393

Parkhurst DL, Appelo CAJ (1999) Useŕs Guide to PHREEQC (version 2)-a computer program for speciation, batch-reaction, one-dimensional transport, and inverse geochemical calculations, USGS WRI Report 99–4259, Washington

Piqué A, Canals A, Grandia F, Banks DA (2008) Mesozoic fluorite veins in NE Spain record regional base metal-rich brine

circulation through basin and basement during extensional events. Chem Geol 257:139–152

Plante B, Benzaazoua M, Bussière B (2011) Predicting geochemical behaviour of waste rock with low acid generating potential using laboratory kinetic tests. Mine Water Environ 30:2–21

Plumlee GS, Smith KS, Montour MR, Ficklin WH, Mosier EL (1999) Geologic controls on the composition of natural waters and mine waters. In: Filipek LH, Plumlee GS (eds) The environmental geochemistry of mineral deposits, Part B: case studies and research topics, reviews in economic geology, vol 6B. MI, Chelsea, pp 373–432

Preis W, Gamsjäger H (2001) Solid + solute) phase equilibria in aqueous solution XIII. Thermodynamic properties of hydrozincite and predominance diagrams for (Zn^{2+}+H_2O + CO_2. J Chem Thermodyn 33:803–819

Reche J, Martínez FJ (2002) Evolution of bulk composition, mineralogy, strain style and fluid flow during an HT-LP metamorphic event: sillimanite zone of the Catalan Coastal Ranges Variscan basement, NE Iberia. Tectonophysics 348:111–134

SAIC (2003) An assessment of laboratory leaching tests for predicting the impacts of fill material on ground water and surface water quality. Toxic Cleanup Program, Olympia

Seal RR, Foley NK (2002) Progress on geoenvironmental models for selected mineral deposit types. USGS Open-File Report 02–195, Washington

Seal RR, Hammarstrom JM (2003) Geoenvironmental models of mineral deposits: examples from massive sulfide and gold deposits. In: Jambor JL, Blowes DW, Ritchie AIM (eds) Environmental aspects of mine wastes. Mineralogical Assoc of Canada, Short Course Series 31, Amerstdam

Seal RR, Hammarstrom JM, Johnson AN, Piatak NM, Wandless GA (2008) Environmental geochemistry of a Kuroko-type massive sulfide deposit at the abandoned Valzinco mine, Virginia, USA. Appl Geochem 23:320–342

Viladevall M, Fondevilla M, Puigserver D, Carmona JM, Cortés A, Navarro A (2007) Poplar trees used for the detection of hazardous elements: case history of the Ebro, Llobregat and Ter valleys (NE, Spain). In: Loredo J (ed), Proc, 23rd International Geochemistry Symp (IAGS), p 145–146

Wehrer M, Totsche KV (2003) Detection of non-equilibrium contaminant release in soil columns: delineation of experimental conditions by numerical simulations. J Plant Nutr Soil Sc 166:475–483

Wehrer M, Totsche KV (2005) Determination of effective release rates of polycyclic aromatic hydrocarbons and dissolved organic carbon by column outflow experiments. European J Soil Sci 56:803–813

Wehrer M, Totsche KV (2008) Effective rates of heavy metal release from alkaline wastes—Quantified by column outflow experiments and inverse simulations. J Contam Hydrol 101:53–66

Younger PL (2000) Nature and practical implications of heterogeneities in the geochemistry of zinc-rich, alkaline mine waters in an underground F–Pb mine in the UK. Appl Geochem 15:1383–1397